

Arbutin-modified microspheres prevent osteoarthritis progression by mobilizing local anti-inflammatory and antioxidant responses



Jiale Jin^{a,1}, Yang Liu^{b,1}, Chao Jiang^{a,1}, Yifan Shen^a, Guangyu Chu^a, Can Liu^a, Lejian Jiang^a, Guanrui Huang^a, Yifang Qin^c, Yijian Zhang^{b,**}, Chi Zhang^{a,*}, Yue Wang^{a,***}

^a Spine Lab, Department of Orthopedic Surgery, The First Affiliated Hospital, Zhejiang University School of Medicine, Hangzhou, 310003, China

^b Department of Orthopaedics, The First Affiliated Hospital of Soochow University, Soochow University, Suzhou, 215006, China

^c Department of Endocrinology, Children's Hospital, Zhejiang University School of Medicine, Hangzhou, China

ARTICLE INFO

Keywords:

Arbutin
Osteoarthritis
Inflammation
Oxidative stress
Microsphere

ABSTRACT

Osteoarthritis (OA) is a common degenerative joint disease worldwide and currently there is no effective strategy to stop its progression. It is known that oxidative stress and inflammation can promote the development of OA, and therapeutic strategies against these conditions may alleviate OA. Arbutin (ARB), a major ingredient of the Chinese medicinal herb cowberry leaf, exerts good antioxidant and anti-inflammatory activities yet has not been studied in OA. Here we developed ARB-loaded gelatine methacryloyl-Liposome (GM-Lipo@ARB) microspheres which showed long-term release of ARB and excellent cartilage-targeting effects. The ARB-loaded microspheres effectively reduced the inflammatory response in interleukin (IL)-1 β -treated arthritic chondrocytes. Moreover, the synthesized GM-Lipo@ARB microspheres regulated cartilage extracellular matrix (ECM) homeostasis through anti-inflammation effect via inhibiting NF- κ B signaling and anti-oxidative stress effect via activating Nrf2 pathway. Intra-articular use of GM-Lipo@ARB can effectively reduce inflammation and oxidative stress in the articular cartilage and thus, attenuating OA progression in a mouse model. The study proposed a novel ARB-laden functional microsphere, GM-Lipo@ARB, and demonstrated that this compound may be used as an alternative therapeutics for treating OA.

1. Introduction

Osteoarthritis (OA) is one of the most common degenerative musculoskeletal diseases worldwide, particularly in aging societies. Although various therapeutic strategies have been proposed to relieve pain and improve functions of the inflamed joint [1], currently there is no effective cure available to promote cartilage regeneration or slow down the progression of OA [2]. The lack of efficacious treatment modalities for OA adds heavy economical burdens on families and societies [3]. New strategies which can substantially promote treatment outcomes are urgently needed in OA practice.

IL-1 β , a key inflammatory factor in the pathogenesis of OA, plays an important role in the histological progression of OA [4]. IL-1 β induced

inflammation and catabolism related pathways, such as nuclear factor kappa B (NF- κ B) and nuclear factor-erythroid 2-related factor-2 (Nrf2) signaling, play a major role in OA development [5–7]. Nrf2, a key transcription factor that regulates antioxidant capacity of cells, can also upregulate hemeoxygenase (HO-1) genes to inhibit NF- κ B pathway [8]. Under IL-1 β stimulation, p65, the downstream protein of NF- κ B, will be transferred into the nucleus and trigger inflammation and matrixdegradation. Moreover, Nrf2 pathway can be indirectly activated upon the inhibition of NF- κ B [9,10]. Simultaneous modulation of IL-1 β related signaling thus may be a promising therapeutic strategy for treating OA [11,12].

Arbutin (ARB), a natural antioxidant extracted from the Chinese medicine herb cowberry leaf [13], can suppress inflammation via

* Corresponding author. The Center for Sports Medicine, Department of Orthopedic Surgery, the First Affiliated Hospital, Zhejiang University School of Medicine; and Institute of Sports Medicine of Zhejiang University, Hangzhou, China.

** Corresponding author. Department of Orthopaedics, The First Affiliated Hospital of Soochow University, Suzhou, 215006, Jiangsu, China.

*** Corresponding author. Department of Orthopedic Surgery, The First Affiliated Hospital, Zhejiang University School of Medicine, Hangzhou 310003, Zhejiang, China.

E-mail addresses: yjzhang2013@stu.suda.edu.cn (Y. Zhang), locuszcz@zju.edu.cn (C. Zhang), wangyuespine@zju.edu.cn (Y. Wang).

¹ These authors contributed equally to this work.

inhibiting NF- κ B pathway in animal models of diabetes [14], demyelination [15], and acute lung injury [16]. Moreover, ARB can protect cells against oxidation via activating Nrf2 [17]. Although ARB has been studied in many disorders, the anti-inflammation feature of ARB on chondrocytes and its effects on treating OA have not been explored. Yet, ARB is prone to oxidation and decomposition under acidic condition, as that in an OA joint [18,19]. To overcome these drawbacks, a novel vector is needed to protect ARB from oxidation and achieve sustained release.

Gelatine methacryloyl (GM) is a natural polymer derived from hydrolysed collagen. With biological activities similar to that of collagen, GM has been widely used as a raw material for biological materials [20]. GM microspheres, a natural nanoparticle and a specific type GM with porous features, is often used as a drug delivery platform [21]. On the other hand, Liposomes are self-assembling vesicles which can efficiently encapsulate both water-soluble and fat-soluble drugs [22]. Moreover, the cationic Liposomes are ideal vectors for targeting the negatively charged cartilage [23]. Evidence suggested that functionalized microspheres composed of Liposomes and GM can achieve cartilage-targeting and sustained release of on-demand drug [24]. In theory, anti-inflammatory and antioxidant effects of ARB can be better administered to OA environment in the presence of functional microspheres, and ARB-coated hydrogel may inhibit inflammation in the cartilage and thus, alleviate the progression of OA.

In this study we integrated cationic Liposomes and GM microspheres to develop an ARB-modified microsphere (GM-Lipo@ARB) for treating OA. We demonstrated that this compound can protect cartilage extracellular matrix (ECM) from degradation and ameliorate OA pathologies through regulating inflammation and redox homeostasis via the Nrf2/NF- κ B pathways (Fig. 1).

2. Results

2.1. Synthesis and characterization of GM-Lipo@ARB microspheres

The mixture of GM, liposomes and ARB was cut by Span 80 oil to form uniform droplets, which were cross-linked to form microspheres under UV light. Loading drugs into positive liposomes and packaging them into GM microspheres increases the encapsulation efficiency of the drugs while effectively reducing the release rate of ARB (Fig. 2A). Scanning electron microscopy showed that the liposomes were uniformly distributed on the surface of the GM microspheres (Fig. 2B). The average particle size of the liposomes was less than 200 nm, which facilitated entry into chondrocytes. A PDI of 0.156 indicated that the microspheres showed good dispersion (Fig. 2C), and the zeta potential at +20 mV indicated that they could effectively adsorb negatively charged glycosaminoglycans in chondrocytes (Fig. 2D). FTIR indicated an unaffected composite endowed with liposomes and ARB (Fig. 2E). When placed in a

solution containing 0.2 mg/mL collagenase, the weight of GM-Lipo@ARB decreased by 64.8% compared with that of GM microspheres, which decreased by 72.0% at 28 days, showing a slower in vitro degradation rate (Fig. 2F). In drug release experiments, the cumulative release spectra of GM@ARB, Lipo@ARB, and GM-Lipo@ARB were all bipolar. After three days of rapid release, the release efficiencies of the GM@ARB and Lipo@ARB were 75.6% and 76.3%, which were higher than that of GM-Lipo@ARB (46.1%). In addition, the cumulative release of GM-Lipo@ARB was 67.6% at 28 days, compared with 82.0% for GM@ARB and 81.6% for Lipo@ARB, indicating an excellent sustained-release system (Fig. 2G).

2.2. GM-Lipo@ARB was cell-friendly and showed cartilage-targeting effects

To verify the biocompatibility of the modified microspheres, micro-morphology, cell proliferation, and cell viability assays were performed on the cell-microsphere complex. Microscopy images indicated that the cells grew steadily with the microspheres after five days of coculture (Fig. 3A). CCK8 analysis showed that the microspheres had no effect on chondrocyte proliferation at any time point (Fig. 3B). Moreover, when cells grew with the microspheres, quantitative analysis indicated no significant difference in the percentage of live cells between each group (Fig. 3C and D).

In this study, a red fluorescence signal was observed in chondrocytes after they were incubated with Deere-labelled cationic liposomes (Fig. 3E), indicating that the cationic liposomes had been absorbed by chondrocytes. As shown in Fig. 3F, DiI-labelled liposomes were used to examine liposome attachment to the cartilage surface, and red fluorescence was distributed on the cartilage surface, confirming the cartilage-targeting property of the liposomes. Cationic liposomes can interact with negatively charged cells and are easily internalized by them.

2.3. GM-Lipo@ARB maintained cartilage ECM homeostasis

An in vitro arthritic environment was established by treatment with the classical proinflammatory factor interleukin (IL)-1 β . Immunofluorescence staining showed that GM-Lipo@ARB could effectively promote the expression of the synthetic marker Collagen II (Col II) and suppress the activity of the matrix degrading enzyme MMP13 in IL-1 β -treated chondrocytes (Fig. 4A and B). Then, the results were analyzed (Fig. 4C). Intriguingly, the cells that grew with the microspheres exhibited a consistent trend, as evidenced by the enhanced ECM anabolism level in the GM-Lipo@ARB group (Fig. 4D-F). Western blot assays (WB) indicated that GM-Lipo@ARB upregulated the expression of Col II and Aggrecan but decreased the expression of MMP13 and ADAMTS5 (Fig. 4G). Moreover, analysis of the WB results was performed (Fig. S1A).

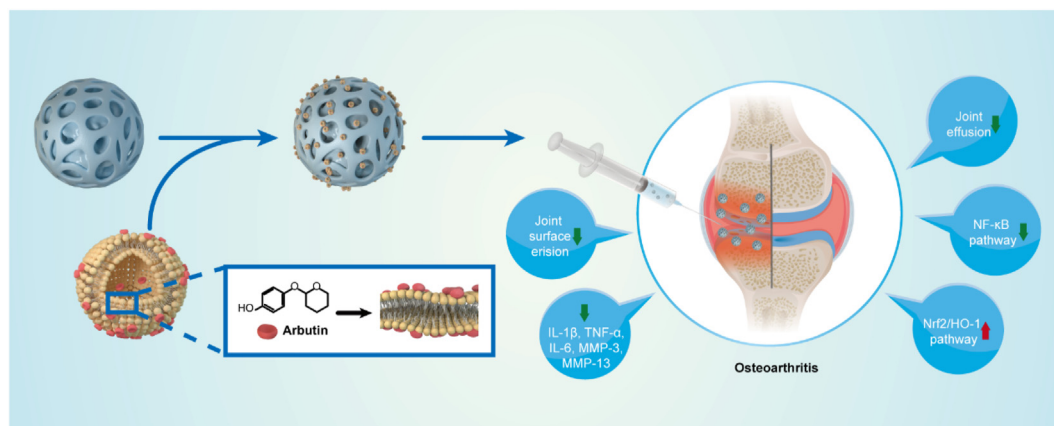


Fig. 1. Composite hydrogel (GM-Lipo@ARB) for the treatment of osteoarthritis.

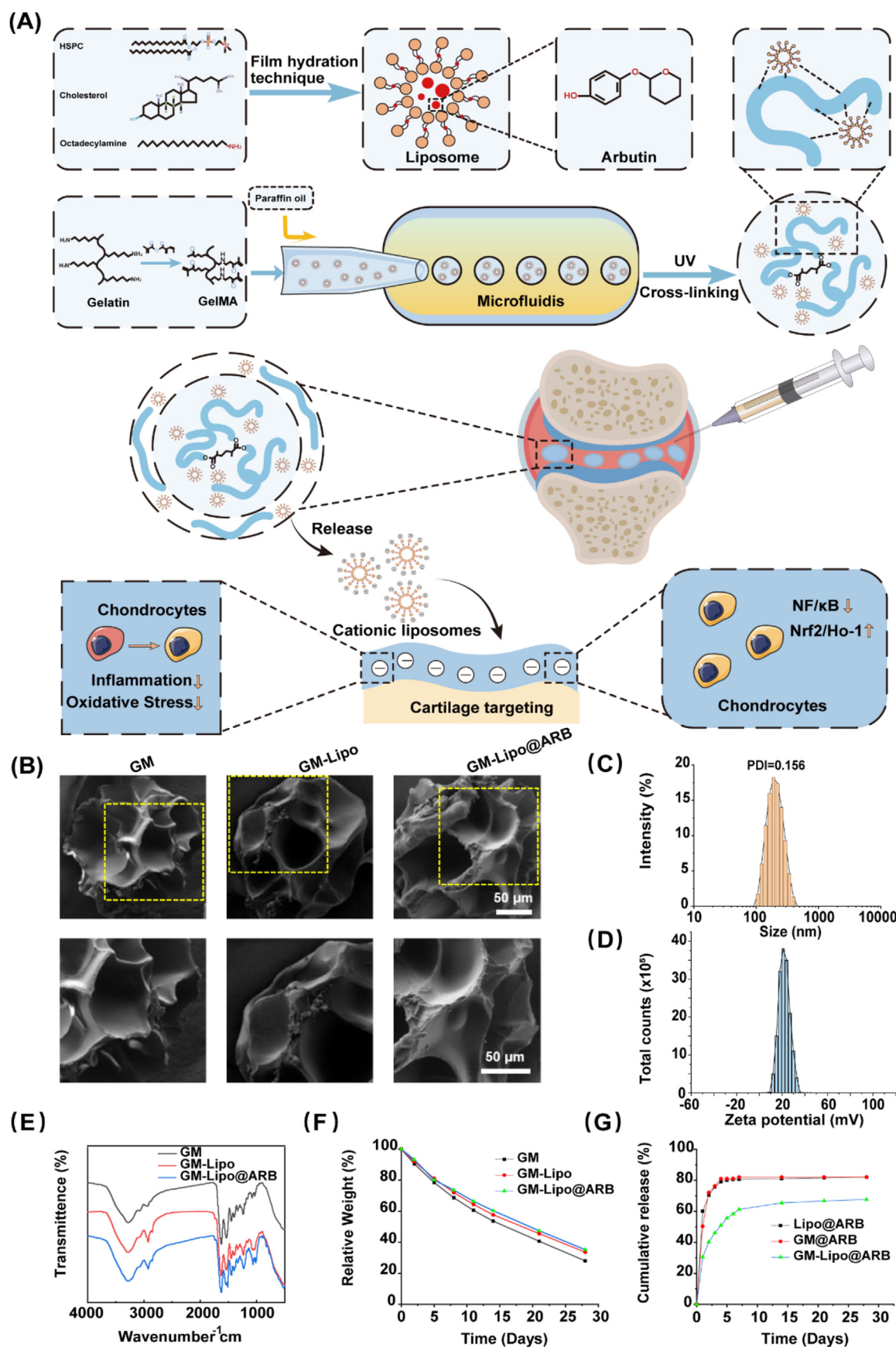


Fig. 2. Synthesis and characterization for GM-Lipo@ARB microspheres. (A) The principle and fabrication of GM-Lipo@ARB. (B) SEM images of GM, GM-Lipo and GM-Lipo@ARB from the overall view and the local view. (C) Size distribution of liposomes. (D) Zeta potential of liposomes. (E) FTIR of GM, GM-Lipo and GM-Lipo@ARB. (F) The degradation curve of GM, GM-Lipo and GM-Lipo@ARB. (G) Release curves of ARB releasing from GM, GM-Lipo and GM-Lipo@ARB.

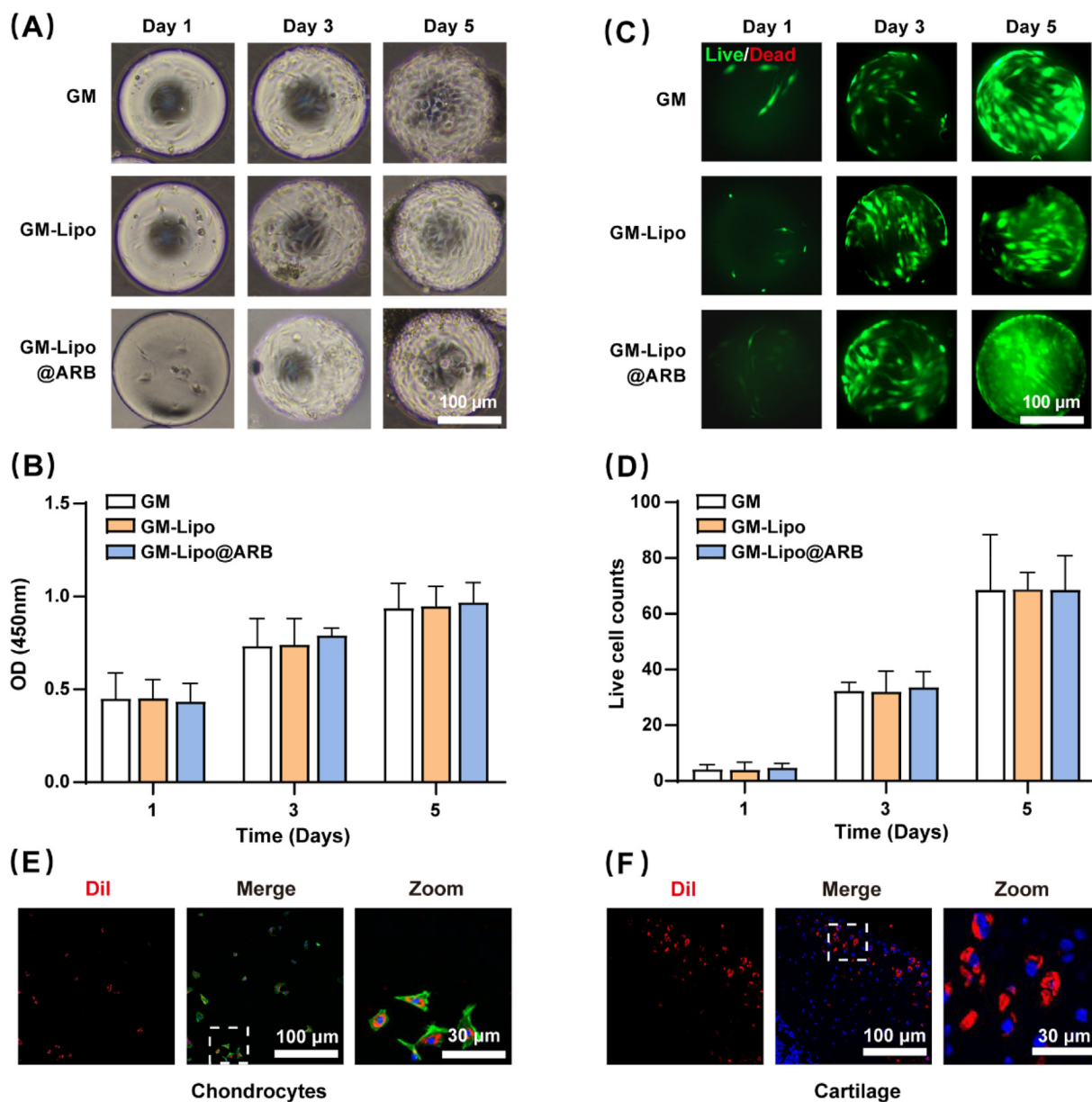


Fig. 3. Biocompatibility and cartilage-targeting of GM-Lipo@ARB. (A) Microscopy images of cells on microspheres after 1, 3, and 5 days of incubation. (B) The CCK-8 results on 1, 3, and 5 days. OD, optical density. (C) Live/dead staining of cells on microspheres after 1, 3, and 5 days of incubation. (D) Viable cell counts from the Live/Dead staining assay. (E) Immunofluorescence of the chondrocytes incubated with Dil-labelled cationic liposomes. (F) Immunofluorescence of the cartilage section incubated with Dil-labelled cationic liposomes.

Quantitative Real-time PCR (RT-PCR) further corroborated the positive regulation of GM-Lipo@ARB on cartilage ECM equilibrium (Fig. 4J).

2.4. GM-Lipo@ARB inhibited the inflammatory response via the NF- κ B axis

RT-PCR showed that GM-Lipo@ARB decreased the expression levels of iNOS, COX-2, tumour necrosis factor (TNF)- α , and IL-6, all of which participated in the generation and development of the inflammatory cascade (Fig. 5A). Subsequent WB and ELISA experiments confirmed the inhibitory effect of the released ARB on the local inflammatory micro-environment (Fig. 5B and C). Meanwhile, analysis of the WB results was performed (Fig. S2A). Immunofluorescence staining revealed that IL-1 β -mediated production of iNOS was alleviated by treatment with GM-Lipo@ARB (Fig. 5D). Immunofluorescence analysis was performed for iNOS (Fig. S2B). The potential mechanisms of ARB-modified

microspheres that yielded anti-inflammatory effects were further analyzed. WB indicated that the protein level of p65 was reduced in GM-Lipo@ARB-treated cells; however, the I κ B α protein level was elevated, indicating inhibition of NF- κ B dimers in the cytoplasm (Fig. 5E). Furthermore, analysis of the WB results was performed (Fig. S2C). In addition, immunofluorescence stain verified that the nuclear translocation of p65 was comprehensively blocked following GM-Lipo@ARB treatment (Fig. 5F). Immunofluorescence analysis was performed for p65 (Fig. S2D). Similar results were confirmed by immunofluorescence for I κ B α (Fig. S2E).

2.5. GM-Lipo@ARB regulated on both inflammation and redox status via Nrf2 and NF- κ B pathway

Molecular docking experiments indicated that Nrf2 may act as a target protein of ARB (Fig. 6A), the remaining set of result is presented in

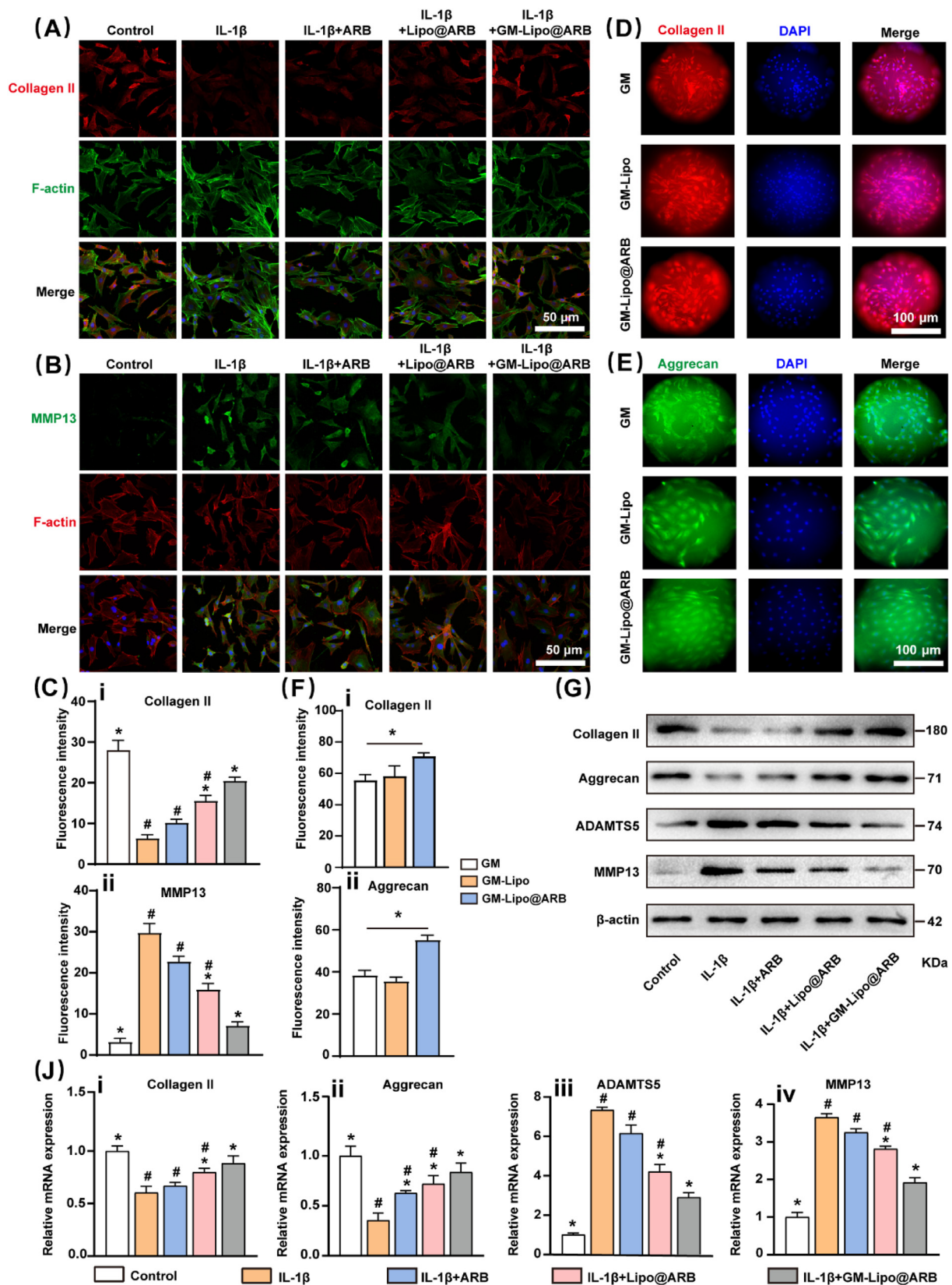


Fig. 4. Effects of GM-Lipo@ARB on ECM homeostasis. (A, B) Immunofluorescence images of Col II and MMP13 protein. (C) Quantification of Col II and MMP13 fluorescences. (n = 3, # and * indicate P < 0.05 in comparison with the control and IL-1 β groups, respectively) (D, E) Immunofluorescence images of Col II and Aggrecan on cells that grew with the microspheres. (F) Quantification of Col II and MMP13 fluorescences on microspheres. (n = 3, * indicate P < 0.05) (G) Western blot of ECM proteins and ECM degrading enzymes. (J) Protein expression result of ECM proteins (i-ii) and ECM degrading enzymes (iii-iv) by semi-quantification (n = 3, # and * indicate P < 0.05 in comparison with the control and IL-1 β groups, respectively).

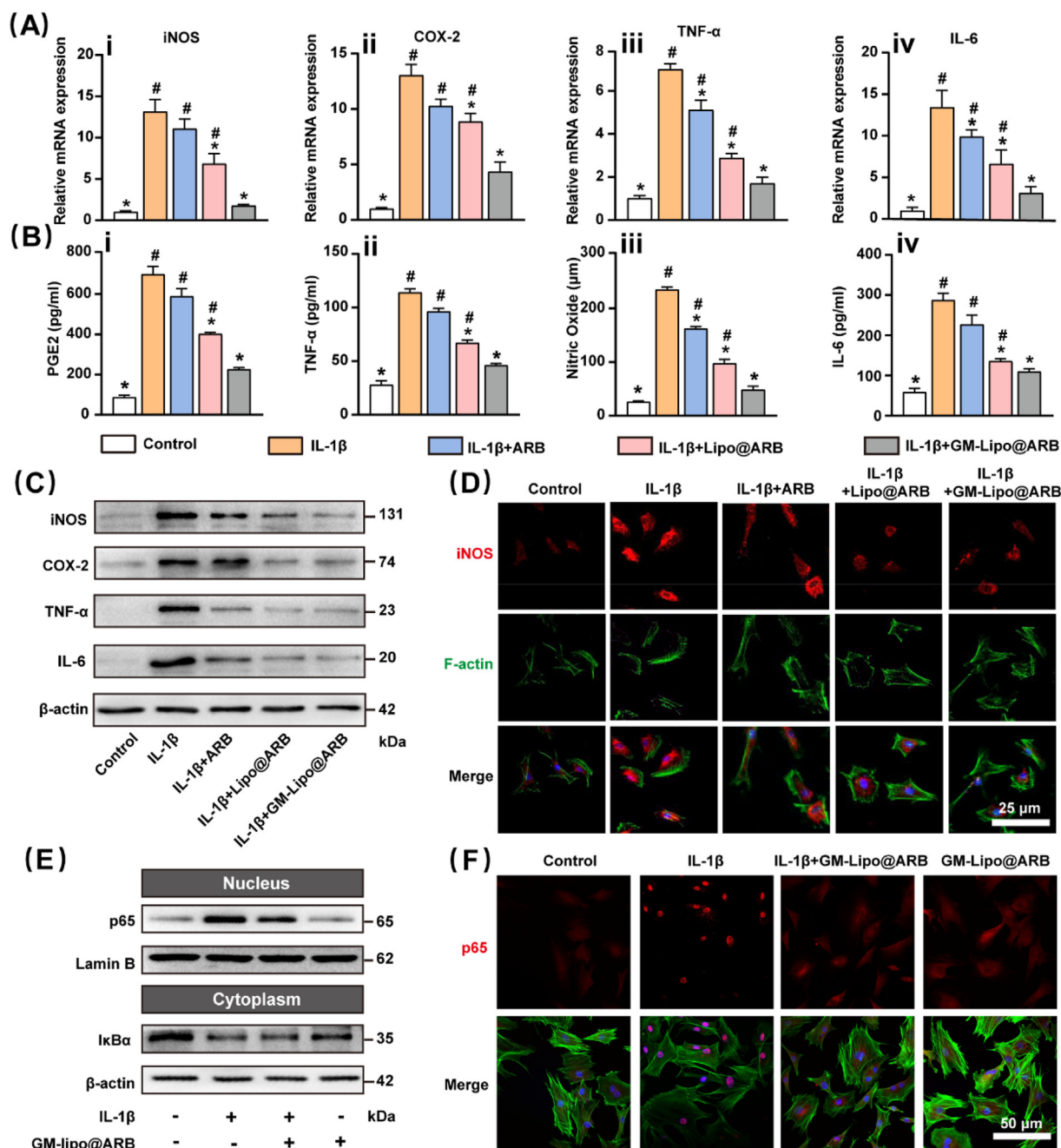


Fig. 5. Effects of GM-Lipo@ARB on inflammation. (A) RT-PCR results showing the levels of (i) iNOS, (ii) COX-2, (iii) TNF-α, and (iv) IL-6. (B) ELISA results showing the levels of (i) PGE2, (ii) TNF-α, (iii) Nitric Oxide, and (iv) IL-6. (C) Western blot of inflammatory protein and inflammatory factor. (D) Immunofluorescence images of iNOS protein. (E) Western blot of NF-κB signaling pathway. (F) Immunofluorescence images of p65 protein. (n = 3, # and * indicate P < 0.05 in comparison with the control and IL-1β groups, respectively).

the supplementary materials (Figs. S3A–C). Nrf2 plays an indispensable role in modulating redox balance by binding the antioxidant response element sequence in the nucleus. WB indicated that the Nrf2-HO-1 axis was activated by the modified microspheres (Fig. 6B). Results from WB were statistically analyzed in Fig. S3E. Immunofluorescence staining also indicated that the nuclear translocation of Nrf2 was increased by GM-Lipo@ARB (Fig. 6C) and the results were statistically analyzed (Fig. S3F). Consistently, immunofluorescence staining of HO-1 confirmed the antioxidant effect of GM-Lipo@ARB (Fig. S3D).

Moreover, Nrf2-specific siRNA was transfected into GM-Lipo@ARB-treated cells, and Nrf2-specific siRNA knockdown was confirmed by WB (Figs. S4A–B). Furthermore, insufficiency of Nrf2 impaired the protective effect of GM-Lipo@ARB on cartilage ECM homeostasis (Fig. 6D).

Supplementary Fig. S3G presented the statistical results of WB. More importantly, Nrf2 inhibition activated the NF-κB-mediated inflammatory pathway, as indicated by increased p65 protein levels (Figs. S5A–B), reducing the anti-inflammatory effect of GM-Lipo@ARB (Fig. 6F).

Then this study further blocked the downstream protein p65 via NF-κB inhibitor (BAY-11-7082). While Nrf2 and HO-1 were enhanced, the nuclear translocation of p65 was almost eliminated under Bay-11-7082 treatment (Figs. S5C–D). Moreover, inhibition of NF-κB pathway improved the antioxidant capacity of GM-Lipo@ARB on chondrocytes (Figs. S5E–F). The above results indicated a regulatory effect of GM-Lipo@ARB on both inflammation and redox status.

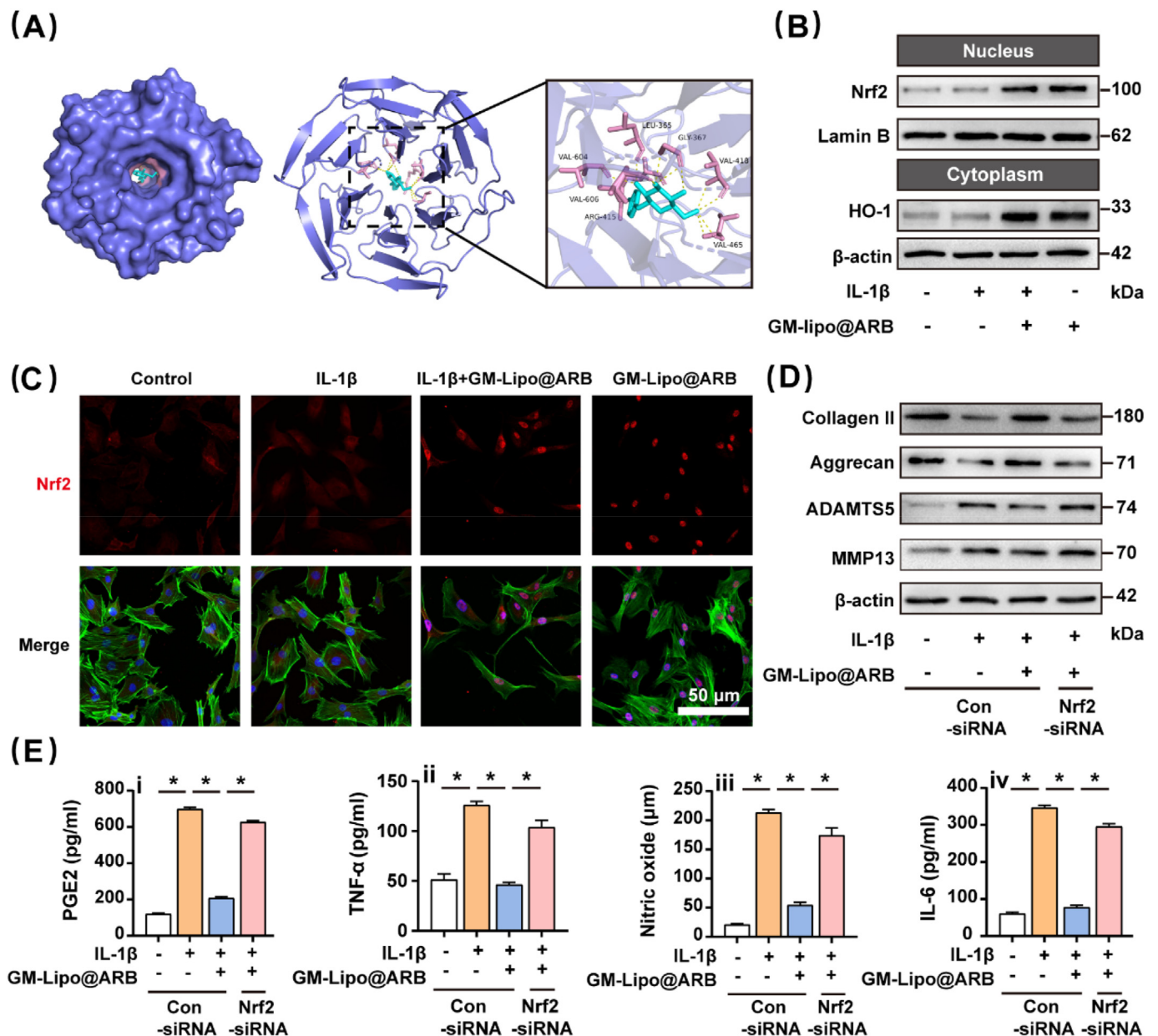


Fig. 6. Effects of GM-Lipo@ARB on oxidative stress. (A) The reaction between ARB and Nrf2 complex (B) Western blot of Nrf2/HO-1 signaling pathway. (C) Immunofluorescence images of Nrf2 protein. (D) Western blot of ECM proteins and ECM degrading enzymes under siRNA. (E) ELISA results showing the levels of (i) PGE2, (ii) TNF-α, (iii) Nitric Oxide, and (iv) IL-6. (n = 3, * indicate P < 0.05).

2.6. Intra-articular injection of GM-Lipo@ARB delayed OA progression

The in vivo effect of GM-Lipo@ARB on cartilage degeneration in experimental OA mice were investigated. Intra-articular injection of GM-Lipo@ARB preserved the expression of glycosaminoglycan in articular cartilage, as shown by H&E and safranin O staining (Fig. 7A and B). Similarly, the OARSI score was decreased by treatment with ARB-modified microspheres (Fig. 7F). Moreover, immunohistochemical analysis showed that GM-Lipo@ARB increased the expression of Col II but decreased the expression of MMP13 in hyaline cartilage in destabilization of the medial meniscus (DMM)-impaired mice (Figs. S6A–C), indicating improved protective potency against ECM metabolism in vivo. More specifically, as shown in the immunofluorescence assay, the transcription factor Nrf2 was significantly increased while the inflammatory factor iNOS was efficiently suppressed following the injection of ARB-laden microspheres (Fig. 7C and D). Additionally, 8-hydroxy-2'-deoxyguanosine (8-OHdG) was an iconic marker of oxidative damage, Fig. 7E

shows the results of immunohistochemistry for 8-OHdG and the anti-oxidation effect of GM-Lipo@ARB. The corresponding statistical results are reported in Fig. 7F. These results demonstrated that GM-Lipo@ARB exerted dual regulatory effects on inflammation and oxidative stress balance and prevented OA progression in vivo by activating the Nrf2 pathway.

3. Discussion

In this study, ARB was loaded into the cationic Liposomes to obtain long-term stability and cartilage-targeting capability. GM microspheres were then incorporated with ARB-loaded Liposomes (GM-Lipo@ARB) to achieve a sustained release of ARB. We demonstrated that GM-Lipo@ARB can attenuate IL-1β-induced oxidative stress and inflammation in mouse chondrocytes, and alleviate OA pathologies in a mouse model via activating Nrf2 and inhibiting NF-κB signaling.

Overactivated inflammatory response in OA is regarded as the major

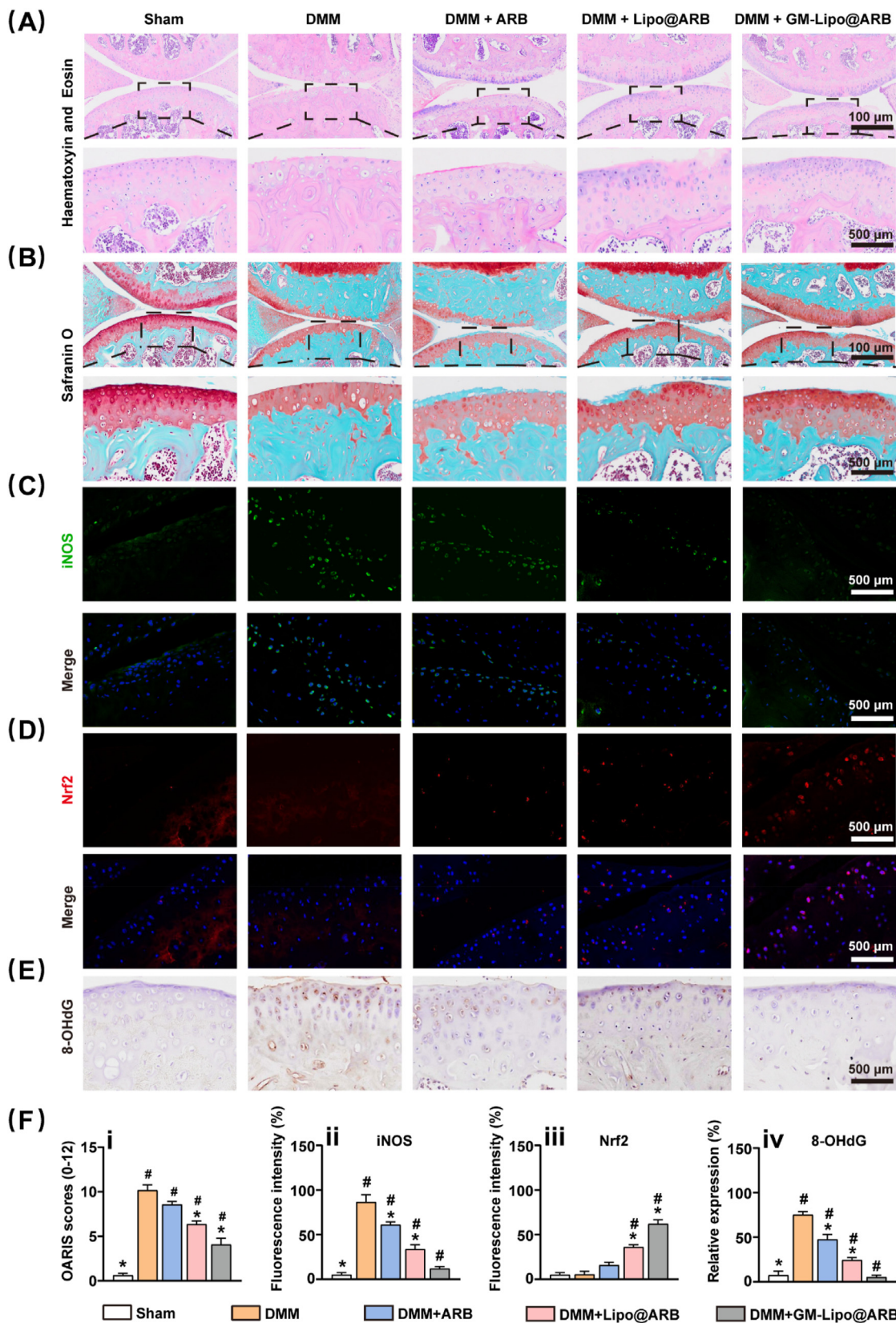


Fig. 7. Effects of GM-Lipo@ARB on OA in vivo. (A) Representative images of HE staining for each group. (B) Representative images of Safranin O-fast green staining for each group. (C) Images of iNOS protein immunofluorescence staining. (D) Images of Nrf2 protein immunofluorescence staining. (E) Images of 8-OHdG protein immunohistochemical staining. (F) Quantification analysis of (i) OARIS score, (ii) relative iNOS expression (iii) relative Nrf2 expression, and (iv) relative 8-OHdG expression. (n = 7, # and * indicate P < 0.05 in comparison with the sham and DMM groups, respectively).

driver in the progression of OA [25]. Although anti-inflammatory drugs can alleviate pain symptoms, they cannot arrest the progression of endogenous inflammation in OA patients [26]. Previous studies have demonstrated that ARB as a natural product had a robust anti-inflammatory effect in animal models of epilepsy [27], lung injury [28], and cardiac hypertrophy [29]. Adding to previous knowledge, this study illustrated that ARB can suppress inflammation in OA via inhibiting p65 nuclear translocation in NF- κ B signaling. Besides, the ARB-induced NAD-dependent protein deacetylase sirtuin 1 (SIRT1) can inhibit apoptosis and autophagy, and then reduce the secretion of inflammatory cytokines [30]. Our previous study found that the pineal-produced hormone melatonin can rescue IL-1 β - or TNF- α -impaired chondrogenic potential in synovial mesenchymal stem cells via activating SIRT1 [31]. Therefore, the crosstalk between ARB and SIRT1 deserves further investigation.

Consisting of superoxide anions, hydrogen peroxide, and hydroxyl radicals, reactive oxygen species (ROS) are mainly produced in oxidative phosphorylation reactions in the mitochondria [32]. Accumulation of ROS may impair cartilage redox equilibrium and activate matrix proteinases [33]. In addition to anti-inflammation property, our study found that ARB had promising antioxidant property by enhancing the expression of the redox-sensitive element Nrf2 and its downstream antioxidant enzyme HO-1. Strengthening the Nrf2-HO-1 pathway not only alleviated oxidative stress insults, but also enhanced anabolic metabolism in ECM to against OA. Interestingly, some upstream mediators of Nrf2 may also be targets of ARB [34–37]. While enhance Nrf2 signaling can improve the expression of catalase and superoxide dismutase and arrest the overproduction of ROS [38], Nrf2 deficiency can deteriorate the function of mitochondrial antioxidant enzymes and impair mitochondrial respiration [39]. Impact of ARB on the mitochondrial function thus may be an important mechanism through which ARB exert therapeutic effects.

There were complicated crosstalks between NF- κ B and Nrf2 signaling [40,41]. A major one occurs between NF- κ B/p65 subunit and Nrf2, which compete for the common-activator cAMP response element binding protein (CREBP) -binding protein (CBP) [42,43]. When the NF- κ B pathway was activated in inflammation, NF- κ B/p65 deprives CREBPs from Nrf2, leading to suppressed Nrf2 transcriptional activity [44]. On the other hand, inhibition of NF- κ B pathway can effectively improve Nrf2 transcription into the nucleus [45,46]. While Nrf2-deficient cells had increased NF- κ B/p65 protein levels [47], many studies have illustrated that Nrf2 has an antagonistic effect on the NF- κ B pathway [48,49]. In this study, the interaction between Nrf2 and NF- κ B/p65 involved in GM-Lipo@ARB treatment was explored and an antagonistic role of Nrf2 in the NF- κ B pathway was confirmed.

We developed an injectable microsphere drug delivery system where ARB was packaged in Liposomes and then integrated with GM microspheres. Cationic Liposomes can selectively adhere to the cartilage with little diffusion to synovial tissues. Furthermore, the positively charged Liposome can penetrate into the cartilage matrix and gradually release ARB to regulate the cartilaginous inflammation-redox balance. With long-term release of ARB and excellent biocompatibility, the ARB-modified microspheres showed remarkable repair functions both in vitro and in vivo. Similar to a porous peptide-cell-hydrogel microsphere which can decrease the inflammatory cytokine storms in disc degeneration development [50], the compound GM-Lipo@ARB can decrease inflammatory cytokines in vitro and presented efficient anti-inflammatory effects in OA model mice. While the injury-inflammation-oxidative stress vicious cycle is important in the progression of OA [51], ARB-modified microspheres can scavenge excessive ROS via the Nrf2-HO-1 signaling and thus, break this cycle [52]. Hence, we demonstrated that the developed GM-Lipo@ARB had dual regulations of inflammation and redox and thus, had robust effects of attenuating cartilage degeneration.

In conclusion, this study demonstrated that GM-Lipo@ARB reduces ECM degradation in mouse chondrocytes. Mechanisms underlying the protective effect involve anti-inflammation via inhibiting NF- κ B activation and anti-oxidative stress via activating Nrf2 pathway. Intra-articular

use of GM-Lipo@ARB can effectively reduce inflammation and oxidative stress in the articular cartilage and thus, attenuating OA progression. Findings indicated that GM-Lipo@ARB may be used as an alternative therapeutics for treating OA.

4. Material and methods

4.1. Preparation and characterization of liposomes

Liposomes were prepared via a film dispersion method. In short, HPSC (Aladdin, China), cholesterol and octylamine (Aladdin, China) were dissolved in chloroform at a ratio of 40:10:2. The solution was completely dried by rotary evaporator at 60 °C. The liposomes then extruded through 0.45 μ m and 0.22 μ m membrane filters (Millex, Ireland). Finally, the size distribution, PDI and Zeta potential of liposomes were measured by Malvin Zeta potential and nano particle size analyzer.

4.2. Fabrication and characterization of GM-Lipo@ARB

The mixture of GM 10 wt %, Liposome and photoinitiator was cut by 5 wt % Span 80 oil to form uniform droplets in microfluidic device, which were cross-linked by ultraviolet (UV) irradiation. The liposomes were encapsulated in GM microspheres and the cross-linked microspheres were cleaned with 75% ethanol and stored in deionized water. The size and shape of the microspheres were observed under a light microscope. The structure of the freeze-dried microspheres was observed by scanning electron microscopy (SEM).

4.3. Encapsulation and drug release

The encapsulation rate of ARB was measured by ultraviolet spectrophotometer. Drug release was then measured. In simple terms, GM-Lipo@ARB was loaded into a dialysis bag (MWCO, 1000 kDa) and immersed in a 37 °C PBS solution at 60 rpm for continuous stirring until complete drug release. The drug release at a specific time point was measured by UV spectrophotometer and PBS was replaced with the equivalent volume.

4.4. Degradation tests

A total of 100 mg GM-Lipo/GM/GM-Lipo@ARB lyophilized particles were soaked in 0.2 mg/mL collagenase solution. Microspheres were taken out every two days to measure the remaining solid weight and re-soaked into collagenase solution. Compare the remaining solid weight to the initial weight.

4.5. Cell biocompatibility

Mice chondrocytes from C57BL/6 mice will be used throughout the study. In order to test the biocompatibility of GM-Lipo@ARB, chondrocytes were inoculated on the surface of microspheres and the growth of the cells was observed under a light microscope at 1, 3 and 5 days. Cell proliferation was detected by live/dead staining. Cells were incubated with calcein -AM/propidium iodide (Beyotime, China) for 30 min and examined using a fluorescence microscope.

4.6. Cell culture and transfection

Detailed information is provided in the Supplementary data.

4.7. Immunofluorescence staining

Col II, Aggrecan, MMP13, iNOS, p65, I κ B α , Nrf2 and HO-1 protein levels were detected by immunofluorescence staining. In a nutshell, cells or tissues were immobilised with 4% paraformaldehyde for 15 min and

treated with 2% bovine serum albumin for 1 h to reduce background noise. Cells or tissues were labelled with antibody overnight at 4 °C and then incubated with fluorescent secondary antibody (Servicebio, China) for 2 h. Nuclear staining with DAPI (Servicebio, China) 15 min. The cytoskeleton was stained with phalloidin (Servicebio, China) 1 h. The samples were viewed using Confocal Microscope.

4.8. RT-PCR

Detailed information is provided in the Supplementary data.

4.9. Enzyme-linked immunosorbent assay

Chondrocyte supernatants were measured by ELISA kit (Becton, Dickinson and Company) following the manufacturer's instructions.

4.10. Western blot assay

Detailed information is provided in the Supplementary data.

4.11. The dosage of GM-Lipo@ARB in cells and mouse

The microspheres were intra-articularly injected once every 2 weeks with 10 µL of PBS, ARB (25 mg/kg), Lipo@ARB (25 mg/kg of ARB), and GM-Lipo@ARB (25 mg/kg of ARB) [27,53]. And the chondrocytes were cocultured with ARB (0.5 mg/mL), Lipo@ARB (0.5 mg/mL of ARB), GM-Lipo@ARB (0.5 mg/mL of ARB)/PBS [54].

4.12. Mice model and treatment

C57BL/6 J male mice (6–8 weeks) were purchased from Suzhou Healthytech Bio-pharmaceutical Co, Ltd. (Suzhou, China). All mice were maintained in a SPF (specific-pathogen-free) environment with free access to water and diets under the standard of 12 h-light and 12 h-dark cycle at 22 ± 1 °C. OA model of knee joint was established by surgical destruction of medial meniscus (DMM). Mice were first anesthetized with a mixture of 2.0% isoflurane and 30% oxygen (RWD Life Sciences, Shenzhen, China). The medial meniscus ligament (MML) of OA group was cut with microscissors. In the sham operation group, only the knee capsule was exposed and the integrity of MML was not affected. One week after surgery, the mice were randomly divided into 5 groups. Control, PBS, ARB, Lipo@ARB and GM-Lipo@ARB microspheres were injected into the joint cavity of the mice.

4.13. Histology and immunohistochemistry staining

Eight weeks after the operation, the mice were euthanized and the isolated knee joint was fixed with paraformaldehyde, decalcified and paraffin embedded. Sagittal sections with a thickness of 5 mm were histologically analyzed by HE and Saffron O-fast green staining and grading the degree of cartilage degeneration according to the Osteoarthritis Research Society International (OARSI) scoring system. For immunohistochemical staining, sections were incubated with Col II/MMP13/8-OHdG antibody at 4 °C overnight and then incubated with secondary antibody for 1 h. Then, the tissue sections were stained with 3, 3'-diaminobenzidine substrates. The relative expression levels of Col II, MMP13 and 8-OHdG were quantified by Image J software.

4.14. Statistical analysis

Each work was carried out at least three times via GraphPad Prism (Version 8.4.3, CA). One-way analysis of variance (ANOVA) with Tukey's post hoc test were used for multiple comparisons, and student's t tests were used to compare means of two groups. All Data are presented as mean ± SEM. P < 0.05 was considered statistically significant.

Credit author statement

Yue Wang, Chi Zhang, Yijian Zhang designed the research; **Jiale Jin, Yang Liu, and Chao Jiang** conducted the experiments **in vitro and in vivo**; **Guanrui Huang, Yifan Shen and Guangyu Chu** prepared the figures. **Liu Can, Lejian Jiang and Yifang Qin** analyzed the data; **Jiale Jin and Chi Zhang** wrote the paper. All authors contributed to the article and approved the submitted version. **Jiale Jin**: Methodology, Investigation, Writing - Original Draft, Writing - Review & Editing. **Yang Liu**: Methodology. **Chao Jiang**: Methodology. **Yifan Shen**: Visualization. **Guangyu Chu**: Visualization. **Can Liu**: Formal analysis. **Lejian Jiang**: Formal analysis. **Guanrui Huang**: Visualization. **Yifang Qin**: Formal analysis. **Yijian Zhang**: Conceptualization, Writing - Review & Editing. **Chi Zhang**: Conceptualization, Resources, Writing - Original Draft, Writing - Review & Editing, Supervision. **Yue Wang**: Conceptualization, Writing - Review & Editing.

Declarations

Ethics approval and consent to participate

All animal experiments and studies were guided and approved by the Ethics Committee of the First Affiliated Hospital of Zhejiang University.

Availability of data and materials

All datasets used and analyzed in this article can be obtained from the corresponding author on reasonable grounds.

Consent for publication

Not applicable.

Conflicts of interest

No potential conflicts of interest were identified.

Funding

This work was funded by National Natural Science Foundation of China (82002320), Natural Science Foundation of Zhejiang Province (LQ21H060005) and Science Technology Department of Zhejiang Province (2020C03042).

Declaration of competing interest

The authors declare the following financial interests/personal relationships which may be considered as potential competing interests:

Chi Zhang reports financial support was provided by National Natural Science Foundation of China. Chi Zhang reports financial support was provided by Natural Science Foundation of Zhejiang Province. Yue Wang reports financial support was provided by Science Technology Department of Zhejiang Province.

Acknowledgements

Not applicable.

Appendix A. Supplementary data

Supplementary data to this article can be found online at <https://doi.org/10.1016/j.mtbio.2022.100370>.

References

- [1] J.N. Katz, K.R. Arant, R.F. Loeser, Diagnosis and treatment of hip and knee osteoarthritis: a review, *JAMA* 325 (6) (2021) 568–578, <https://doi.org/10.1001/jama.2020.22171>.
- [2] Q. Ji, X. Xu, L. Kang, Y. Xu, J. Xiao, S.B. Goodman, X. Zhu, W. Li, J. Liu, X. Gao, Z. Yan, Y. Zheng, Z. Wang, W.J. Maloney, Q. Ye, Y. Wang, Hematopoietic PBX-interacting protein mediates cartilage degeneration during the pathogenesis of osteoarthritis, *Nat. Commun.* 10 (1) (2019) 313, <https://doi.org/10.1038/s41467-018-08277-5>.
- [3] H. Long, Q. Liu, H. Yin, K. Wang, N. Diao, Y. Zhang, J. Lin, A. Guo, Prevalence Trends of Site-specific Osteoarthritis from 1990 to 2019: Findings from the Global Burden of Disease Study 2019, *Arthritis & rheumatology*, Hoboken, N.J., 2022, <https://doi.org/10.1002/art.42089>.
- [4] T. Matsuzaki, O. Alvarez-Garcia, S. Mokuda, K. Nagira, M. Olmer, R. Gamini, K. Miyata, Y. Akasaki, A.I. Su, H. Asahara, M.K. Lotz, FoxO transcription factors modulate autophagy and proteoglycan 4 in cartilage homeostasis and osteoarthritis, *Sci. Transl. Med.* 10 (428) (2018), <https://doi.org/10.1126/scitranslmed.aan0746>.
- [5] K. Manthiram, Q. Zhou, I. Akseptijevich, D.L. Kastner, The monogenic autoinflammatory diseases define new pathways in human innate immunity and inflammation, *Nat. Immunol.* 18 (8) (2017) 832–842, <https://doi.org/10.1038/ni.3777>.
- [6] H. Kabata, K. Moro, S. Koyasu, The group 2 innate lymphoid cell (ILC2) regulatory network and its underlying mechanisms, *Immunol. Rev.* 286 (1) (2018) 37–52, <https://doi.org/10.1111/immr.12706>.
- [7] G. Tang, S. Li, C. Zhang, H. Chen, N. Wang, Y. Feng, Clinical efficacies, underlying mechanisms and molecular targets of Chinese medicines for diabetic nephropathy treatment and management, *Acta Pharm. Sin. B* 11 (9) (2021) 2749–2767, <https://doi.org/10.1016/j.apsb.2020.12.020>.
- [8] H. Sies, C. Berndt, D.P. Jones, Oxidative stress, *Annu. Rev. Biochem.* 86 (2017) 715–748, <https://doi.org/10.1146/annurev-biochem-061516-045037>.
- [9] H.F. Zhang, J.H. Wang, Y.L. Wang, C. Gao, Y.T. Gu, J. Huang, J.H. Wang, Z. Zhang, Salvianolic acid A protects the kidney against oxidative stress by activating the akt/GSK-3 β /nrf2 signaling pathway and inhibiting the NF- κ B signaling pathway in 5/6 nephrectomized rats, *Oxid. Med. Cell. Longev.* 2019 (2019), 2853534, <https://doi.org/10.1155/2019/2853534>.
- [10] J.A. Leite, T.J. Isaksen, A. Heuck, C. Scavone, K. Lykke-Hartmann, The α (2) Na(+)/K(+)-ATPase isoform mediates LPS-induced neuroinflammation, *Sci. Rep.* 10 (1) (2020), 14180, <https://doi.org/10.1038/s41598-020-71027-5>.
- [11] H. Chen, J. Qin, H. Shi, Q. Li, S. Zhou, L. Chen, Rhoifolin ameliorates osteoarthritis via the Nrf2/NF- κ B axis: in vitro and in vivo experiments, *Osteoarthritis Cartilage* 30 (5) (2022) 735–745, <https://doi.org/10.1016/j.joca.2022.01.009>.
- [12] J. Jin, X. Lv, B. Wang, C. Ren, J. Jiang, H. Chen, X. Chen, M. Gu, Z. Pan, N. Tian, A. Wu, L. Sun, W. Gao, X. Wang, X. Zhang, Y. Wu, Y. Zhou, Limonin inhibits IL-1 β -induced inflammation and catabolism in chondrocytes and ameliorates osteoarthritis by activating Nrf2, *Oxid. Med. Cell. Longev.* 2021 (2021), 7292512, <https://doi.org/10.1155/2021/7292512>.
- [13] H.J. Lee, K.W. Kim, Anti-inflammatory effects of arbutin in lipopolysaccharide-stimulated BV2 microglial cells, *Inflamm. Res.* : official journal of the European Histamine Research Society ... [et al.] 61 (8) (2012) 817–825, <https://doi.org/10.1007/s00011-012-0474-2>.
- [14] L. Lv, J. Zhang, F. Tian, X. Li, D. Li, X. Yu, Arbutin protects HK-2 cells against high glucose-induced apoptosis and autophagy by up-regulating microRNA-27a, *Artif. Cell Nanomed. Biotechnol.* 47 (1) (2019) 2940–2947, <https://doi.org/10.1080/21691401.2019.1640231>.
- [15] M. Saeedi, K. Khezri, A. Seyed Zakaryaei, H. Mohammadamini, A comprehensive review of the therapeutic potential of α -arbutin, *Phytother. Res.* 35 (8) (2021) 4136–4154, <https://doi.org/10.1002/ptr.7076>.
- [16] M. Kumar, A. Kumar, R.K. Sindhu, A.S. Kushwah, Arbutin attenuates monosodium L-glutamate induced neurotoxicity and cognitive dysfunction in rats, *Neurochem. Int.* 151 (2021), 105217, <https://doi.org/10.1016/j.neuint.2021.105217>.
- [17] Y.C. Boo, Arbutin as a skin depigmenting agent with antimelanogenic and antioxidant properties, *Antioxidants* 10 (7) (2021), <https://doi.org/10.3390/antiox10071129>.
- [18] X. Wu, G. Ren, R. Zhou, J. Ge, F.H. Chen, The role of Ca(2+) in acid-sensing ion channel 1a-mediated chondrocyte pyroptosis in rat adjuvant arthritis, *Laboratory investigation; a journal of technical methods and pathology* 99 (4) (2019) 499–513, <https://doi.org/10.1038/s41374-018-0135-3>.
- [19] T. Jin, D. Wu, X.M. Liu, J.T. Xu, B.J. Ma, Y. Ji, Y.Y. Jin, S.Y. Wu, T. Wu, K. Ma, Intracellular delivery of celastrol by hollow mesoporous silica nanoparticles for pH-sensitive anti-inflammatory therapy against knee osteoarthritis, *Journal of Nanobiotechnology* 18 (1) (2020) 94, <https://doi.org/10.1186/s12951-020-00651-0>.
- [20] B. Kong, Y. Chen, R. Liu, X. Liu, C. Liu, Z. Shao, L. Xiong, X. Liu, W. Sun, S. Mi, Fiber reinforced GelMA hydrogel to induce the regeneration of corneal stroma, *Nat. Commun.* 11 (1) (2020) 1435, <https://doi.org/10.1038/s41467-020-14887-9>.
- [21] Z. Yuan, X. Yuan, Y. Zhao, Q. Cai, Y. Wang, R. Luo, S. Yu, Y. Wang, J. Han, L. Ge, J. Huang, C. Xiong, Injectable GelMA cryogel microspheres for modularized cell delivery and potential vascularized bone regeneration, *Small* 17 (11) (2021), e2006596, <https://doi.org/10.1002/sml.202006596>.
- [22] C.H. Chen, S.M. Kuo, Y.C. Tien, P.C. Shen, Y.W. Kuo, H.H. Huang, Steady augmentation of anti-osteoarthritic actions of rapamycin by liposome-encapsulation in collaboration with low-intensity pulsed ultrasound, *Int. J. Nanomed.* 15 (2020) 3771–3790, <https://doi.org/10.2147/ijn.S252223>.
- [23] Y.B. Kim, K.T. Zhao, D.B. Thompson, D.R. Liu, An anionic human protein mediates cationic liposome delivery of genome editing proteins into mammalian cells, *Nat. Commun.* 10 (1) (2019) 2905, <https://doi.org/10.1038/s41467-019-10828-3>.
- [24] S. Mehrotra, R.D. Singh, A. Bandyopadhyay, G. Janani, S. Dey, B.B. Mandal, Engineering microsphere-loaded non-mulberry silk-based 3D bioprinted vascularized cardiac patches with oxygen-releasing and immunomodulatory potential, *ACS Appl. Mater. Interfaces* 13 (43) (2021) 50744–50759, <https://doi.org/10.1021/acsami.1c14118>.
- [25] M. Kapoor, J. Martel-Pelletier, D. Lajeunesse, J.P. Pelletier, H. Fahmi, Role of proinflammatory cytokines in the pathophysiology of osteoarthritis, *Nature reviews, Rheumatology* 7 (1) (2011) 33–42, <https://doi.org/10.1038/nrrheum.2010.196>.
- [26] B.R. da Costa, T.V. Pereira, P. Saadat, M. Rudnicki, S.M. Iskander, N.S. Bodmer, P. Bobos, L. Gao, H.D. Kiyomoto, T. Montezuma, M.O. Almeida, P.S. Cheng, C.A. Hincapié, R. Hari, A.J. Sutton, P. Tugwell, G.A. Hawker, P. Jüni, Effectiveness and safety of non-steroidal anti-inflammatory drugs and opioid treatment for knee and hip osteoarthritis: network meta-analysis, *BMJ (Clinical research ed.)* 375 (2021) n2321, <https://doi.org/10.1136/bmj.n2321>.
- [27] S.R. Ahmadian, M. Ghasemi-Kasman, M. Pouramir, F. Sadeghi, Arbutin attenuates cognitive impairment and inflammatory response in pentylenetetrazol-induced kindling model of epilepsy, *Neuropharmacology* 146 (2019) 117–127, <https://doi.org/10.1016/j.neuropharm.2018.11.038>.
- [28] J. Ye, M. Guan, Y. Lu, D. Zhang, C. Li, C. Zhou, Arbutin attenuates LPS-induced lung injury via Sirt1/Nrf2/NF- κ Bp65 pathway, *Pulm. Pharmacol. Therapeut.* 54 (2019) 53–59, <https://doi.org/10.1016/j.pupt.2018.12.001>.
- [29] N. Nalban, R. Sangaraju, S. Alavala, S.M. Mir, M.K. Jerald, R. Sista, Arbutin attenuates isoproterenol-induced cardiac hypertrophy by inhibiting TLR-4/NF- κ B pathway in mice, *Cardiovasc. Toxicol.* 20 (3) (2020) 235–248, <https://doi.org/10.1007/s12012-019-09548-3>.
- [30] C. Ma, D. Zhang, Q. Ma, Y. Liu, Y. Yang, Arbutin inhibits inflammation and apoptosis by enhancing autophagy via SIRT1, *Adv. Clin. Exp. Med. : official organ Wrocław Medical University* 30 (5) (2021) 535–544, <https://doi.org/10.17219/acem/133493>.
- [31] J. Yan, X. Chen, C. Pu, Y. Zhao, X. Liu, T. Liu, G. Pan, J. Lin, M. Pei, H. Yang, F. He, Synovium stem cell-derived matrix enhances anti-inflammatory properties of rabbit articular chondrocytes via the SIRT1 pathway, *Mater Sci Eng C Mater Biol Appl* 106 (2020), 110286, <https://doi.org/10.1016/j.msec.2019.110286>.
- [32] Y. Yang, P. Shen, T. Yao, J. Ma, Z. Chen, J. Zhu, Z. Gong, S. Shen, X. Fang, Novel role of circRSU1 in the progression of osteoarthritis by adjusting oxidative stress, *Theranostics* 11 (4) (2021) 1877–1900, <https://doi.org/10.7150/thno.53307>.
- [33] P.R. Coryell, B.O. Diekmann, R.F. Loeser, Mechanisms and therapeutic implications of cellular senescence in osteoarthritis, *Nat. Rev. Rheumatol.* 17 (1) (2021) 47–57, <https://doi.org/10.1038/s41584-020-00533-7>.
- [34] M. Hou, Y. Zhang, X. Zhou, T. Liu, H. Yang, X. Chen, F. He, X. Zhu, Kartogenin prevents cartilage degradation and alleviates osteoarthritis progression in mice via the miR-146a/NRF2 axis, *Cell Death Dis.* 12 (5) (2021) 483, <https://doi.org/10.1038/s41419-021-03765-x>.
- [35] M. Mao, L. Yang, J. Hu, B. Liu, X. Zhang, Y. Liu, P. Wang, H. Li, Oncogenic E3 ubiquitin ligase NEDD4 binds to KLF8 and regulates the microRNA-132/NRF2 axis in bladder cancer, *Exp. Mol. Med.* 54 (1) (2022) 47–60, <https://doi.org/10.1038/s12276-021-00663-2>.
- [36] L. Wang, K. Bayanbold, L. Zhao, Y. Wang, A. Adamcakova-Dodd, P.S. Thorne, H. Yang, B.H. Jiang, L.Z. Liu, Redox sensitive miR-27a/b/Nrf2 signaling in Cr(VI)-induced carcinogenesis, *Sci. Total Environ.* 809 (2022), 151118, <https://doi.org/10.1016/j.scitotenv.2021.151118>.
- [37] J. Chen, J.Q. Liang, Y.F. Zhen, L. Chang, Z.T. Zhou, X.J. Shen, DCAF1-targeting microRNA-3175 activates Nrf2 signaling and inhibits dexamethasone-induced oxidative injury in human osteoblasts, *Cell Death Dis.* 12 (11) (2021) 1024, <https://doi.org/10.1038/s41419-021-04300-8>.
- [38] X. Zhou, Y. Zhang, M. Hou, H. Liu, H. Yang, X. Chen, T. Liu, F. He, X. Zhu, Melatonin prevents cartilage degradation in early-stage osteoarthritis through activation of miR-146a/NRF2/HO-1 Axis, *J. Bone Miner. Res.* 37 (5) (2022) 1056–1072, <https://doi.org/10.1002/jbmr.4527>.
- [39] M. Cano, S. Datta, L. Wang, T. Liu, M. Flores-Bellver, M. Sachdeva, D. Sinha, J.T. Handa, Nrf2 deficiency decreases NADPH from impaired IDH shuttle and pentose phosphate pathway in retinal pigmented epithelial cells to magnify oxidative stress-induced mitochondrial dysfunction, *Aging Cell* 20 (8) (2021), e13444, <https://doi.org/10.1111/acel.13444>.
- [40] F. Sivandzade, S. Prasad, A. Bhalerao, L. Cucullo, NRF2 and NF- κ B interplay in cerebrovascular and neurodegenerative disorders: molecular mechanisms and possible therapeutic approaches, *Redox Biol.* 21 (2019), <https://doi.org/10.1016/j.redox.2018.11.017>.
- [41] Y. Li, L. Liu, P. Sun, Y. Zhang, T. Wu, H. Sun, K.W. Cheng, F. Chen, Fucoxanthinol from the diatom *nitzschia laevis* ameliorates neuroinflammatory responses in lipopolysaccharide-stimulated BV-2 microglia, *Mar. Drugs* 18 (2) (2020), <https://doi.org/10.3390/md18020116>.
- [42] M.A. Skowron, G. Niegisch, P. Albrecht, G. van Koeveering, A. Romano, P. Albers, W.A. Schulz, M.J. Hoffmann, Various mechanisms involve the nuclear factor (Erythroid-Derived 2)-like (NRF2) to achieve cytoprotection in long-term cisplatin-treated urothelial carcinoma cell lines, *Int. J. Mol. Sci.* 18 (8) (2017), <https://doi.org/10.3390/ijms18081680>.
- [43] N. Farfán, J. Carril, M. Redel, M. Zamorano, M. Araya, E. Monzón, R. Alvarado, N. Contreras, A. Tapia-Bustos, M.E. Quintanilla, F. Ezquer, J.L. Valdés, Y. Israel, M. Herrera-Marschitz, P. Morales, Intranasal administration of mesenchymal stem cell secretome reduces hippocampal oxidative stress, neuroinflammation and cell

- death, improving the behavioral outcome following perinatal asphyxia, *Int. J. Mol. Sci.* 21 (20) (2020), <https://doi.org/10.3390/ijms21207800>.
- [44] A.M. Mahmoud, E.M. Desouky, W.G. Hozayen, M. Bin-Jumah, E.S. El-Nahass, H.A. Soliman, A.A. Farghali, Mesoporous silica nanoparticles trigger liver and kidney injury and fibrosis via altering TLR4/NF- κ B, JAK2/STAT3 and Nrf2/HO-1 signaling in rats, *Biomolecules* 9 (10) (2019), <https://doi.org/10.3390/biom9100528>.
- [45] K.J. Min, J.T. Lee, E.H. Joe, T.K. Kwon, An I κ B α phosphorylation inhibitor induces heme oxygenase-1(HO-1) expression through the activation of reactive oxygen species (ROS)-Nrf2-ARE signaling and ROS-PI3K/Akt signaling in an NF- κ B-independent mechanism, *Cell. Signal.* 23 (9) (2011) 1505–1513, <https://doi.org/10.1016/j.cellsig.2011.05.013>.
- [46] M. Yu, H. Li, Q. Liu, F. Liu, L. Tang, C. Li, Y. Yuan, Y. Zhan, W. Xu, W. Li, H. Chen, C. Ge, J. Wang, X. Yang, Nuclear factor p65 interacts with Keap1 to repress the Nrf2-ARE pathway, *Cell. Signal.* 23 (5) (2011) 883–892, <https://doi.org/10.1016/j.cellsig.2011.01.014>.
- [47] J. Lin, J. Chen, Z. Zhang, T. Xu, Z. Shao, X. Wang, Y. Ding, N. Tian, H. Jin, S. Sheng, W. Gao, Y. Lin, X. Zhang, X. Wang, Luteoloside inhibits IL-1 β -induced apoptosis and catabolism in nucleus pulposus cells and ameliorates intervertebral disk degeneration, *Front. Pharmacol.* 10 (2019) 868, <https://doi.org/10.3389/fphar.2019.00868>.
- [48] D.C. Zhu, Y.H. Wang, J.H. Lin, Z.M. Miao, J.J. Xu, Y.S. Wu, Maltol inhibits the progression of osteoarthritis via the nuclear factor-erythroid 2-related factor-2/heme oxygenase-1 signal pathway in vitro and in vivo, *Food Funct.* 12 (3) (2021) 1327–1337, <https://doi.org/10.1039/d0fo02325f>.
- [49] S. Tang, Q. Tang, J. Jin, G. Zheng, J. Xu, W. Huang, X. Li, P. Shang, H. Liu, Polydatin inhibits the IL-1 β -induced inflammatory response in human osteoarthritic chondrocytes by activating the Nrf2 signaling pathway and ameliorates murine osteoarthritis, *Food Funct.* 9 (3) (2018) 1701–1712, <https://doi.org/10.1039/c7fo01555k>.
- [50] J. Bian, F. Cai, H. Chen, Z. Tang, K. Xi, J. Tang, L. Wu, Y. Xu, L. Deng, Y. Gu, W. Cui, L. Chen, Modulation of local overactive inflammation via injectable hydrogel microspheres, *Nano Lett.* 21 (6) (2021) 2690–2698, <https://doi.org/10.1021/acs.nanolett.0c04713>.
- [51] D. Chen, D. Lu, H. Liu, E. Xue, Y. Zhang, P. Shang, X. Pan, Pharmacological blockade of PCAF ameliorates osteoarthritis development via dual inhibition of TNF- α -driven inflammation and ER stress, *EBioMedicine* 50 (2019) 395–407, <https://doi.org/10.1016/j.ebiom.2019.10.054>.
- [52] J. Li, F. Han, J. Ma, H. Wang, J. Pan, G. Yang, H. Zhao, J. Zhao, J. Liu, Z. Liu, B. Li, Targeting endogenous hydrogen peroxide at bone defects promotes bone repair, *Adv. Funct. Mater.* 32 (10) (2021), <https://doi.org/10.1002/adfm.202111208>.
- [53] P. Chen, C. Xia, S. Mei, J. Wang, Z. Shan, X. Lin, S. Fan, Intra-articular delivery of sinomenium encapsulated by chitosan microspheres and photo-crosslinked GelMA hydrogel ameliorates osteoarthritis by effectively regulating autophagy, *Biomaterials* 81 (2016) 1–13, <https://doi.org/10.1016/j.biomaterials.2015.12.006>.
- [54] Y. Han, J. Yang, W. Zhao, H. Wang, Y. Sun, Y. Chen, J. Luo, L. Deng, X. Xu, W. Cui, H. Zhang, Biomimetic injectable hydrogel microspheres with enhanced lubrication and controllable drug release for the treatment of osteoarthritis, *Bioact. Mater.* 6 (10) (2021) 3596–3607, <https://doi.org/10.1016/j.bioactmat.2021.03.022>.